Integration of local motion is normal in amblyopia

Robert F. Hess and Behzad Mansouri

McGill Vision Research Unit, 687 Pine Avenue West, Room H4-14, Montreal, H3A 1A1 Quebec, Canada

Steven C. Dakin

Institute of Ophthalmology, University College London, 11-43 Bath Street, London EC1V 9EL, United Kingdom

Harriet A. Allen

School of Psychology, University of Birmingham, Birmingham B15 2TT, United Kingdom

Received July 1, 2005; accepted September 30, 2005; posted December 2, 2005 (Doc. ID 63161)

We investigate the global integration of local motion direction signals in amblyopia, in a task where performance is equated between normal and amblyopic eyes at the single element level. We use an equivalent noise model to derive the parameters of internal noise and number of samples, both of which we show are normal in amblyopia for this task. This result is in apparent conflict with a previous study in amblyopes showing that global motion processing is defective in global coherence tasks [Vision Res. **43**, 729 (2003)]. A similar discrepancy between the normalcy of signal integration [Vision Res. **44**, 2955 (2004)] and anomalous global coherence form processing has also been reported [Vision Res. **45**, 449 (2005)]. We suggest that these discrepancies for form and motion processing in amblyopia point to a selective problem in separating signal from noise in the typical global coherence task.

OCIS codes: 330.5510, 330.7310, 330.4150, 330.5000.

1. INTRODUCTION

Motion processing is a fundamental aspect of vision, being involved in early detection, eye-movement control, visual stabilization, and scene segmentation. It is not at all surprising therefore that a substantial proportion of the visual cortex is devoted to it. Although our understanding of the intricacies of cortical motion processing is still in its infancy, there appears to be initially a two-stage process: the detection of local motion in different parts of the field through cells with localized receptive fields with directional selective properties in V1 (Ref. 1) and a more global processing of these local motions over larger regions of the field in areas of the dorsal, extrastriate pathway including areas MT (V5) and MST.[2,3] Neurons in MT and MST have much larger receptive fields, possibly containing many small subunits that represent V1 inputs[4] with extensive center–surround interactions.[5] The receptive fields of MT neurons are large and fall into two classes with either antagonistic or facilitative surrounds producing sensitivity to local motion boundaries or to global motion direction over a large area, respectively.[6]

The task of choice for investigating MT and other associated areas in the dorsal extrastriate pathway has involved directional judgments for global motion. The stimulus used for these tasks contains localized signal elements moving in a coherent direction combined with a variable proportion of other similar elements moving in random directions (termed noise elements). Sensitivity in such a task is determined by the signal/noise ratio at which the signal direction can be accurately gauged. Sensitivity to global motion is disrupted if area MT/MST is lesioned. This has been shown in monkeys[7–10] and in humans.[11] Abnormalities have been reported in human global motion sensitivity in a large variety of conditions including amblyopia,[12,13] Williams syndrome,[14] autism,[15] developmental dyslexia,[16] and hemiplegia.[17] It has been suggested that the underlying processes exhibit an early maturation, which could account for its greater developmental vulnerability.[18]

Amblyopia is a good example. Although originally thought to involve purely spatial dysfunction,[19,20] recent evidence suggests that humans with amblyopia have defective motion processing.[12,21] There are different forms of amblyopia (i.e., strabismic, anisometropic, and form-deprived), and there is good evidence for different spatial deficits in each[22]; however, one thing that all three subtypes have in common is that each exhibits deficits for global motion processing.[12,13] Furthermore, in a recent study by Simmers *et al.*,[12] it was argued that the deficit for global motion processing is due not to deficient local motion processing in, say, V1 but to impaired global motion processing in MT/MST. This paper aims to clarify just what such a deficit might involve. It has often been loosely assumed that global motion processing solely involves the integration of local motion direction in different parts of the visual field; thus by inference the reduced global motion processing in amblyopia must be due to anomalous global integration of local motion signals. What has been overlooked is that the typical global motion task involves not only integration of local motion but also the segregation of the local motion signal from the spatially coextensive noise. It is not in the best interests of the visual system to blindly integrate all local motion signals, especially when, at threshold conditions, 80% of

them are noise containing no pertinent information. Some degree of segregation of signal from noise is required prior to signal integration. We feel that this latter aspect of the task may be the more important one when it comes to the reduced performance of amblyopic eyes. To test this, we measure the purely integrative capacity of amblyopes representing all three subcategories (i.e., strabismic, anisometropic, and form-deprived) for which global motion deficits have been reported previously by using a similar global motion task. In our task all local motion signals carry relevant information to solve the task, and in this case blind integration of all local motion signals is the optimum strategy. We show in this case that performance is normal in amblyopia. We conclude that the defective global motion processing previously reported in amblyopia may not be due to anomalous motion integration as previously thought but is a consequence of abnormal noise segregation.

2. METHODS

A. Observers

Twenty naive observers (ten amblyopic and ten normal) were tested. The visual acuity in amblyopic eyes ranged from 20/40 to 20/400 (for details see Table 1). Refraction was examined in all observers and appropriately corrected prior to the testing period. Informed consent was obtained from all observers before data collection.

B. Apparatus

A Macintosh G3 computer was used to generate and present the stimuli and collect the data. For programming we used the MATLAB environment (MathWorks Ltd.) and the Psychophysics ToolBox.[23] All stimuli were presented on a 20-in. Sony monitor (Trinitron 520GS). The monitor was calibrated and linearized by using a Graseby S370 photometer and the Video Toolbox[24] package. Pseudo-12-bit contrast accuracy was achieved by using a video attenuator,[25] which combined the RBG outputs of the graphic card (ATI Rage 128) into the G gun. The refresh rate, the mean luminance, and the resolution of the screen were 75 Hz, 33 cd/m^2, and 1152×870 pixels, respectively. The viewing distance was 57 cm from the screen in all experiments. One pixel on the screen corresponded to 0.32 mm, which subtended 2.12 arc min at the viewing distance used. The observers performed the task monocularly, with one eye patched at a time.

C. Stimuli

We studied motion integration by using stimuli comprising arrays of spatially bandpass micropatterns, which were presented on a mid-gray background. The stimuli were randomly distributed within a 6° wide circle, centered on the screen. The presentation time was 500 ms. 128 moving Laplacian-of-Gaussian (∇^2G) blobs (see Fig. 1) were used, which were defined as

$$\nabla^2G(x,y)=\frac{x^2+y^2-2\sigma^2}{2\pi\sigma^6}\exp\left(-\frac{x^2+y^2}{2\sigma^2}\right),$$

where σ represents the space constant. The peak spatial frequency of the blobs was defined as

Table 1. Clinical Details of the Amblyopic Observers Participating in the Experiment[a]

Observer	Age (yr)	Type	Refraction		Acuity	Squint	History, Stereo
ML	20	RE	+1.0 −0.75	90°	20/80	ET 6°	Detected age 5 yr, patching for 2 yr
		mixed	−3.25 DS		20/25		
MA	22	LE	−0.25 DS		20/15	Ortho	Detected age 3 yr, patching for 4 yr, glasses for 8 yr
		aniso	+3.50 −0.50	0°	20/200		
LS	22	BE	−2.00+0.50		20/20	Ortho	Detected age 6 yr, bilateral cataract surgery age 6 yr, patching at 8 yr for 4 m
		depriv	+0.50	90°	20/125		
VD	23	LE	+0.25		20/20	ET 3°	Detected age 5–6 yr, patching for 6 m, no surgery
		mixed	+2.75 −1.25	175°	20/40		
XL	31	LE	−2.50		20/20	ET 15°	Detected age 13 yr, no treatment
		strab	−2.75+0.75	110°	20/400		
PH	33	LE	−2.0+0.50 DS		20/25	ET 5°	Detected age 4 yr, patching for 6 m, surgery at 5 yr
		strab	+0.50 DS		20/63		
ED	43	LE	+0.75		20/16	ET 5°	Detected age 6 yr, patching for 1 yr
		strab	+0.75		20/63		
RB	49	LE	+3.25 DS		20/15	XT 5°	Detected age 6 yr, glasses since 6 yr, no other therapy, near normal local stereovision
		strab	+4.75 −0.75	45°	20/40		
EF	56	LE	+2.00+1.00	180°	20/32	ET 6°	Detected age 6 yr, patching for 1–2 yr, no surgery
		strab	+2.00+1.00	130°	20/250		
VE	69	LE	+4.5 −5.00	30°	20/80	ET 5°	Detected age 10 yr, no treatment
		mixed	−1.75 −1.75	150°	20/25		

[a]Abbreviations: strab, strabismic; aniso, anisometropic; depriv, deprived amblyopia; RE, right eye; LE, left eye; ET, esotropia; XT, exotropia; ortho, orthotropic alignment; DS, diopter sphere.

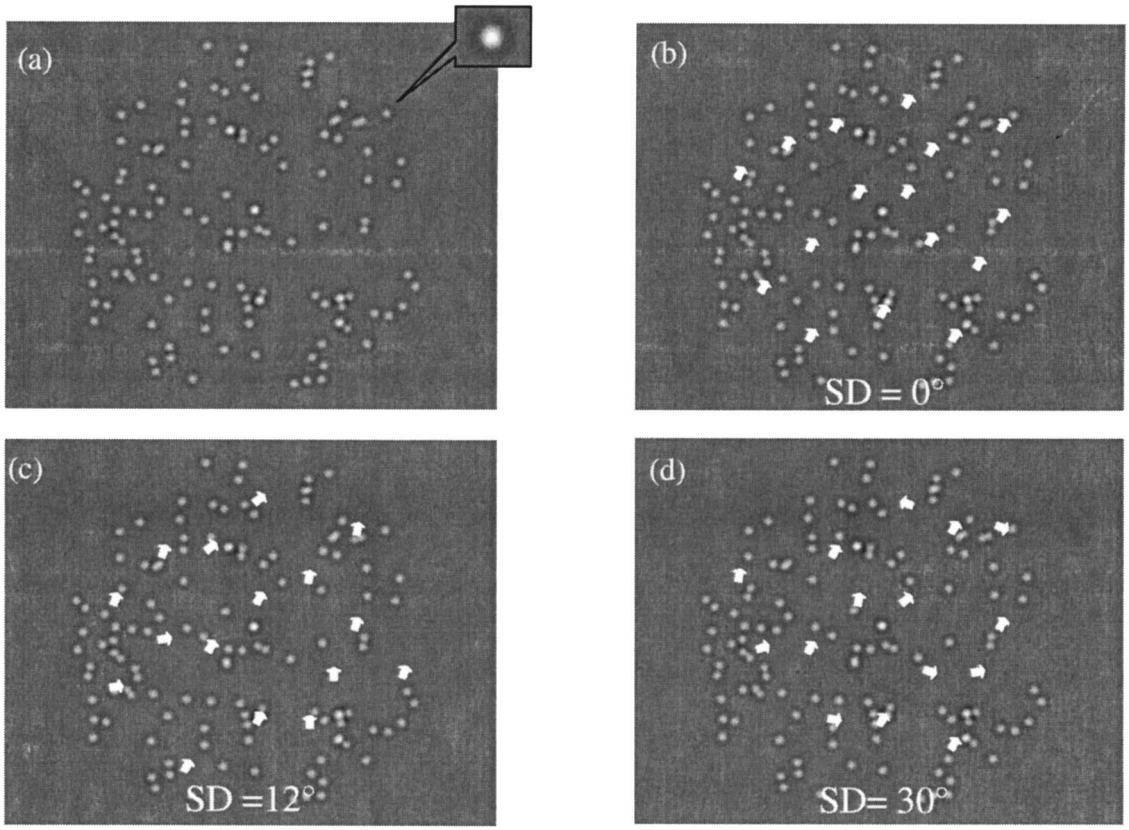

Fig. 1. Illustrations of stimuli used in the experiment. Arrays of 128 randomly positioned, moving blobs were presented in a 6° circle at the center of the screen. The size of a single blob is magnified in (a) for illustration only. The blobs were moving upward and to left or right of vertical. The direction of each element is a sample from a Gaussian distribution of directions with average equal to the cue direction (i.e., 90°± the cue generated by APE) and a variable bandwidth. The white arrows [in (b)–(d)] schematically represent the directions of the blobs. In (b), (c), and (d) the average directions are tilted to right of vertical and the SDs of the stimuli arrays are 0°, 12°, and 30°, respectively.

$$f_{peak} = \frac{1}{\pi\sigma\sqrt{2}}.$$

For this experiment σ was equal to 6.75 arc min, and the peak spatial frequency was 2 c/deg. Each blob was moving upward and to left or right of vertical for the whole presentation time. If a blob passed the border of the presentation window, it was regenerated at the opposite side simultaneously.

The direction of each moving blob was selected from a Gaussian parent distribution with a mean equal to the overall mean direction (i.e., 90°± the cue generated by adaptive probit estimation (APE)[26] and a variable bandwidth. The direction distributions' standard deviation (SD) was varied from 0° (all elements moving in one direction) to 50° (see Fig. 1). Since the motion direction of all elements was selected from the Gaussian parent distribution, all signals contained useful information about the mean of this distribution. Thus the best strategy for the visual system to employ to perform the task involving estimating the mean direction of the array motion would be to integrate motion direction across all elements [see Figs. 1(b)–1(d)].

In the rare cases when the patches overlapped, their gray levels were added and clipped appropriately at the maximum or minimum gray level when they were outside the range of the screen (to see an example of stimuli that we used, go to http://www.mvr.mcgill.ca/Behzad/Motion.html).

D. Statistics

We measured discrimination thresholds for the mean direction of motion in the array and derived the parameters, internal noise (i.n.) and number of samples, (n.s.), from our equivalent noise model, for four groups, namely, the fellow fixing eyes (FFEs) and amblyopic eyes (AMEs) of amblyopic observers and the dominant eyes (DEs) and nondominant eyes (NDEs) of normal observers. There was one factor, namely, the SD of the signal population, having ten levels (0°, 1°, 2°, 4°, 6°, 8°, 12°, 16°, 20°, and 28°). We used the *t*-test to analyze the data. Each group was separately compared with the others. We used a paired *t*-test (repeated-measure *t*-test) when we compared AMEs with FFEs in amblyopic observers and DEs with NDEs in normals. We also calculated 95% confidence intervals (CIs) for the thresholds from each individual psychometric function by using a bootstrapping technique and used it to compare individual sets of data within the groups.

3. PROCEDURE

A. Equating Performance at the Single Element Level

To equate the performance levels for this task at the individual element level for FFEs and AMEs we measured the motion direction discrimination threshold for a single element, of the exact type used in the later integration experiment, as a function of the contrast of the stimulus. This single stimulus element was presented in a random position within the 6° presentation area, the same area as that for the following integration experiment. The direction of a single blob with respect to the notional vertical was measured. The magnitude of the tilt was determined by the APE procedure. A single temporal interval, two-alternative forced choice paradigm was used. Observers had to judge whether the element's motion direction was clockwise or counterclockwise (tilted to right or left of vertical). We used a method of constant stimuli. The observers' direction threshold was estimated from the slope of the best fitting cumulative Gaussian psychometric function derived from between 256 and 512 presentations. 95% CIs were estimated from 1000 bootstrap replications of the fit.[27,28]

In amblyopic observers the single element was presented to the AME with a fixed high contrast (50%) and to the FFE with a range of contrasts. The threshold for the FFE increased with decreasing contrast. Therefore the contrast with which the FFE gave an equal threshold for direction discrimination to that of the AME with the fixed high contrast stimulus was selected. In the subsequent integration experiment the stimuli were presented with contrasts for the FFEs and AMEs that gave comparable thresholds for the single element task.

For our group of normal controls we used stimuli of 25% contrast in the integration experiments. This contrast represents the average contrast level used for the FFEs of amblyopes.

B. Motion Integration

Arrays of 128 randomly positioned, moving blobs were presented. The direction of an individual blob was chosen from a Gaussian distribution with a variable bandwidth and a mean equal to the cue (i.e., 90°± the cue generated by APE). A single temporal interval, two-alternative forced choice paradigm was used. The observers' task was to judge whether the mean direction of the array of blobs was to right or left of vertical. Direction discrimination thresholds were obtained from between 256 and 512 presentations for each SD (ten levels typically between 0° and 50°) of the parent distribution. The motion direction threshold for each level of variability of the parent distribution was estimated from the slope of the best fitting cumulative Gaussian function by using a maximum likelihood procedure. An equivalent noise model[29] was fitted to the thresholds separately for each eye of each observer in each condition.

4. RESULTS

In Fig. 2 results are shown for direction discrimination of a single element for a normal subject and three of our amblyopic subjects (a strabismic, an anisometropic, and a form-deprived amblyope). The threshold for direction discrimination is plotted against the contrast of the element. For amblyopic observers, performance was measured for the AME with a high (50%) contrast element. The contrast used for the FFE was that which gave equivalent performance (indicated by the vertical arrows). The subsequent integration experiments were carried out with element contrasts for which performance was equated at the single element level.

Figure 3 shows sample data sets of thresholds for a normal observer and for each of the three representative amblyopic observers (i.e., strabismic, anisometropic, and form-deprived amblyope) for motion direction integration. The task involved determining the mean direction of the array of element motions with respect to the vertical. The *X* axis is the SD of the signal population, which was varied from 0° to 50° (0°, 1°, 2°, 4°, 8°, 12°, 20°, 30°, 40°, and 50°). The *Y* axis is the motion direction threshold offset (deg). The data are fitted by an equivalent noise model.[29–31] The parameters of internal noise (i.n.) and number of samples (n.s.) are shown in the insets. Increasing the SD beyond a point (at around a SD of 6°) leads to a rise in thresholds. The circles and dashed curves represent the data for the FFE, and the squares and solid curves represent the AME. The AME and FFE show similar thresholds (95% CI, $p > 0.05$). Furthermore, when we compare AMEs with FFEs, the parameters of i.n. and n.s. are not statistically different ($p > 0.05$).

Similar results to these were collected for all normal and amblyopic observers. In all cases the normal observers' DEs and NDEs showed similar performances to those of the FFEs and AMEs of the amblyopic observers.

In Fig. 4 the average values for the parameter of i.n. (*X* axis) are compared for DEs (light gray bar) and NDEs (dark gray bar) of ten normal observers and AMEs (black bar) and FFEs (white bar) of ten amblyopic observers. The i.n. is comparable and not statistically different ($p > 0.05$) among the four groups.

In Fig. 5 the *Y* axis represents the n.s. parameter. This parameter was not statistically different for DEs, NDEs, FFEs, and AMEs either.

5. DISCUSSION

We used a global motion direction task in a group of amblyopes in which direction detection performance was equated at the single element level. This ensured that any deficit that we subsequently measured for subjects estimating the mean direction of the array of element motions had to be due to a deficit at the level of global integration rather than local motion transduction *per se*. Had we not done this and used identical stimuli for testing the normal and amblyopic eyes, any deficit found for our mean direction task could have, in principle, been due to an inability to determine the local motion direction and/or an inability to integrate multiple directions. Performance was measured as a function of the SD of the parent distribution from which the motion direction of individual elements represented samples. We used an equivalent noise model to derive two parameters, one additive [i.e., internal noise (i.n.)] and one multiplicative [i.e., number of samples (n.s.)]. Our results show that amblyopes, be they

strabismic, anisometropic, or form-deprived, exhibit normal integration of motion direction. The i.n. and n.s. were comparable between the normals and amblyopes and between the FFE and the AME of amblyopes. This result is in stark contrast to the abnormal performance of amblyopic observers reported by Ref. 12 for strabismic and anisometropic amblyopes and by Ref. 13 for form-deprived amblyopes in a similar task involving global motion. This is particularly baffling, since the previous study (Ref. 12), also ensured, as we did, that any performance deficit was not due to the encoding of motion at the single element level. Therefore the discrepancy between that study and the present one must pertain to the level at which global motion is analyzed.

A similar discrepancy is present for global form processing. In a subsequent paper (Ref. 32), using a comparable global form task showed that amblyopes exhibit anomalies at the stage of global rather than local form processing. Furthermore, the anomaly for global form processing is greater for second order (i.e., contrast-defined) than for first order (i.e., luminance-defined) stimuli. We have subsequently shown, using a global form task similar to that described here for motion, that global spatial integration of first order[30] and second order[33] stimuli is normal in amblyopia. An understanding of this discrepancy between our finding and those of Simmers and co-workers[12,32] for both form and motion global processing may give us a clue as to where the problem is in amblyopia and possibly why global processing is often found to be abnormal in developmental brain disorders.[34] In our global form and motion tasks, where all the elements contain relevant information about the mean of the distribution to be estimated (mean orientation in the form task and mean direction in the motion task), an ideal observer would blindly integrate all the available information. Amblyopes can do this normally, as we have shown for form tasks[30] and, in this present study, for motion tasks. However, contrast this to the more typical global motion or form coherence task where there is signal as well as noise. In this case an ideal observer would need to segregate signal from noise as well as integrate the signal across space. Indeed there is good evidence that such seg-

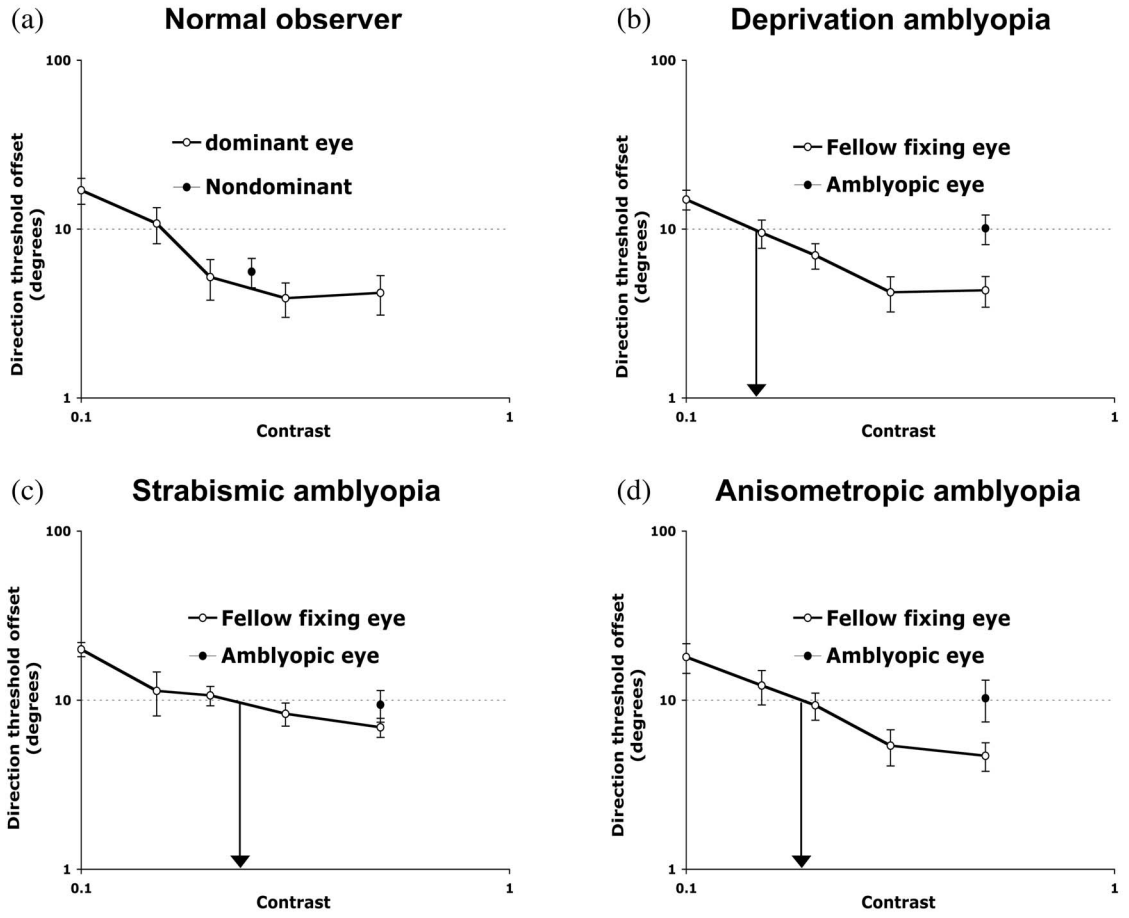

Fig. 2. Matching local direction discrimination in (a) one normal and (b)–(d) three amblyopic observers. The amblyopic categories consisted of (b) deprived amblyopia, (c) strabismic amblyopia, and (d) anisometropic amblyopia. The *X* axis is the contrast of the stimuli, and the *Y* axis is the threshold direction offset for a single moving element. In (a) the open circles and the solid curve represent data for the DE at various contrasts (10%–50%) for one normal observer, and the solid circle for represents the data point for the NDE at 25% contrast. As the contrast of the stimuli decreases, the discrimination threshold increases for the DE. At 25% contrast the thresholds on both eyes are statistically the same (95% CI, $p > 0.05$). In (b)–(d) the open circles and the solid curves represent the data for FFEs. The solid circles represent the thresholds for AMEs at a fixed high contrast of 50%. The arrows show the contrast chosen for elements to be presented to the FFE in the rest of the experiment. This contrast produces equivalent performance to that for the AME when presented with a 50% contrast element. The error bars represent 95% CIs.

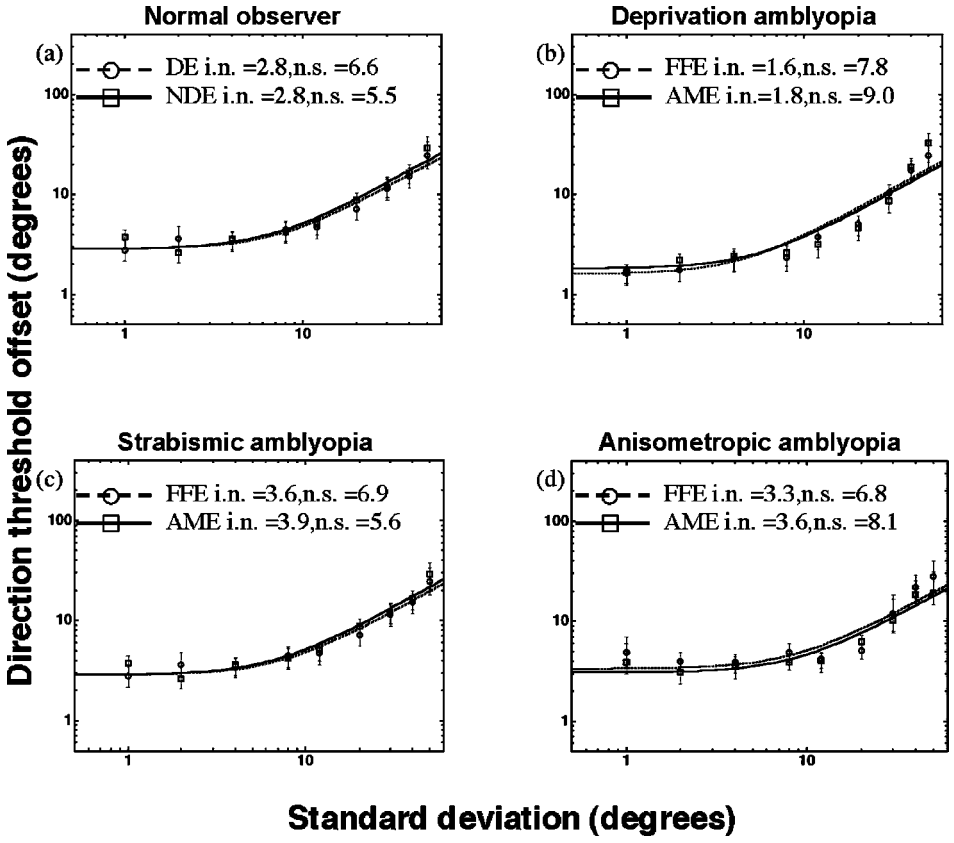

Fig. 3. Motion direction integration threshold measured as a function of the SD (0°–50°) of parent motion direction populations. Circles and dashed curves show the thresholds for (a) the DE of one normal observer and (b)–(d) the FFEs of three amblyopic observers. Squares and solid curves represent the thresholds for (a) the NDE of one normal observer (b)–(d) and the AMEs of three amblyopic observers. The parameters of internal noise (i.n.) and number of samples (n.s.) from the equivalent noise model are shown in insets. The error bars represent 95% CIs.

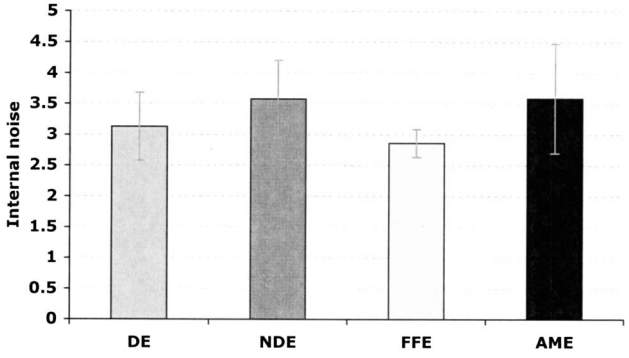

Fig. 4. Average internal noise in ten normal and ten amblyopic observers plotted for DEs (light gray), NDEs (dark gray), FFEs (white), and AMEs (black). The error bars represent ±0.5 SD. The i.n. is statistically similar in all amblyopic and normal observers' eyes ($p > 0.05$).

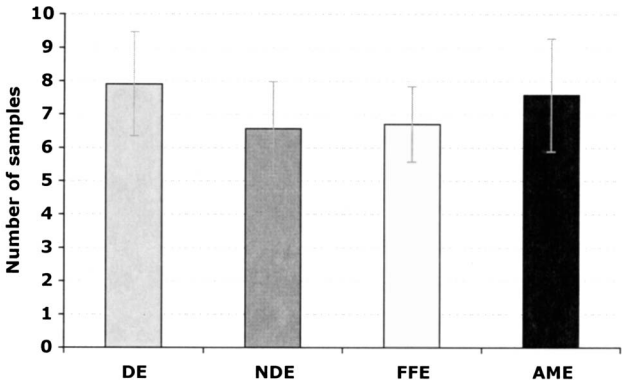

Fig. 5. Average n.s. in ten normal and ten amblyopic observers plotted for DEs (light gray), NDEs (dark gray), FFEs (white), and AME (black). The error bars represent ±0.5 SD. The n.s. is statistically similar in all amblyopic and normal observers' eyes ($p > 0.05$).

regation processes are available to normals because when noise is introduced in a pure integration task of the type used in this study, normals exhibit performance that is much better than that of an ideal observer blindly integrating all signals.[35] For example, in an experiment in which the mean orientation of an array of Gabor elements was to be judged,[35] when half of the elements were noise, the best i.n. estimates for an ideal observer, blindly integrating all elements, were around 19.5, whereas normals in this situation exhibited i.n. estimates of around 2.8. Normal performance is a factor of 7 better than would be expected on the basis of blindly integrating all the available information. Therefore we assume that some, albeit imperfect, form of signal from noise segregation is taking place in normal vision. We speculate that the discrepancy between pure integration global tasks[30,33] and coherence global tasks[12,32] in amblyopia might arise because amblyopes are less able to separate signal from noise in the typical global coherence task.

Deficits to the dorsal stream in the extrastriate cortex that lead to global motion deficits[7] are characterized by profound anomalies to the signal segregation aspect of the task.[11] It will be interesting to know to which of the two complementary extrastriate processes other developmental anomalies (i.e., Williams syndrome, developmental dyslexia, autism) are more vulnerable during development[18]: integration or segregation?

ACKNOWLEDGMENTS

This work was supported by a Canadian Institute of Health Research grant (108-18) to Robert F. Hess. We are grateful to all our amblyopic subjects, who so unselfishly gave up their time for research.

Corresponding author: Behzad Mansouri, McGill Vision Research Unit, 687 Pine Avenue West, Room H4-14, Montreal, Canada H3A1A1. Phone, 514-934-1934, ext. 35307; fax, 514-843-1691; e-mail, behzad.mansouri@mcgill.ca. Website, http://www.mvr.mcgill.ca/Behzad/

REFERENCES

1. D. H. Hubel and T. N. Weisel, "Receptive fields and functional architecture of monkey striate cortex," J. Physiol. (London) **195**, 215–243 (1968).
2. A. Mikami, W. T. Newsome, and R. H. Wurtz, "Motion selectivity in macaque visual cortex. I. Mechanisms of direction and speed selectivity in extra-striate area MT," J. Neurophysiol. **55**, 1308–1327 (1986).
3. A. Mikami, W. T. Newsome, and R. H. Wurtz, "Motion selectivity in macaque visual cortex. II. Spatiotemporal range of directional interactions in MT and V1," J. Neurophysiol. **55**, 1328–1339 (1986).
4. J. A. Movshon, E. H. Adelson, M. S. Gizzi, and W. T. Newsome, "The analysis of moving visual patterns," in *Pattern Recognition Mechanism*, C. Chagas, R. Gattass, and C. Gross, eds. (Vatican Press, 1985), pp. 117–151.
5. J. Allman, F. Miezin, and E. McGuinness, "Direction and velocity specific responses from beyond the classical receptive field in middle temporal visual area (MT)," Perception **14**, 105–126 (1985).
6. R. T. Born and R. B. Tootell, "Segregation of global and local motion processing in primate middle temporal visual area," Nature (London) **357**, 497–499 (1992).
7. W. T. Newsome and E. B. Pare, "A selective impairment of motion perception following lesions of the middle temporal visual area (MT)," J. Neurosci. **8**, 2201–2211 (1988).
8. P. H. Schiller and K. M. Lee, "The effects of lateral geniculate nucleus, area V4 and middle temporal (MT) lesions on visually guided eye movements," Visual Neurosci. **11**, 229–241 (1994).
9. K. Rudolph and T. Pasternak, "Transient and permanent deficits in motion perception after lesions of cortical area MT and MST in macaque monkey," Cereb. Cortex **9**, 90–100 (1999).
10. K. Lauwers, R. Sounders, R. Vogels, E. Vandenbussche, and G. A. Orban, "Impairment in motion discrimination tasks is unrelated to amount of damage to superior temporal sulcus motion area," J. Comp. Neurol. **420**, 539–557 (2000).
11. C. L. Baker, Jr., R. F. Hess, and J. Zihl, "Residual motion perception in a 'motion-blind' patient, assessed with limited-lifetime random dot stimuli," J. Neurosci. **11**, 454–461 (1991).
12. A. J. Simmers, T. Ledgeway, R. F. Hess, and P. V. McGraw, "Deficits to global motion processing in human amblyopia," Vision Res. **43**, 729–738 (2003).
13. D. Ellemberg, T. L. Lewis, D. Maurer, S. Brar, and H. P. Brent, "Better perception of global motion after monocular than after binocular deprivation," Vision Res. **42**, 169–179 (2002).
14. J. Atkinson, O. J. Braddick, S. Anker, W. Curran, R. Andrews, and J. Braddick, "Neurobiological models of visuo-spatial cognition in young William syndrome children: measures of dorsal stream and frontal function," Dev. Neuropsychol. **23**, 139–172 (2003).
15. J. Spencer, J. O'Brien, K. Riggs, O. J. Braddick, J. Atkinson, and J. Wattam-Bell, "Motion processing in autism: evidence for a dorsal-stream deficiency," NeuroReport **11**, 2765–2767 (2000).
16. P. Cornelissen, A. Richardson, A. Mason, S. Fowler, and J. Stein, "Contrast sensitivity and coherent motion detection measured at photopic luminance levels in dyslexics and controls," Vision Res. **35**, 1483–1494 (1995).
17. A. Gunn, E. Cory, J. Atkinson, O. J. Braddick, J. Wattam-Bell, A. Guzzetta, and G. Cioni, "Dorsal and ventral stream sensitivity in normal development and hemiplegia," NeuroReport **13**, 843–847 (2002).
18. O. J. Braddick, J. Atkinson, and J. Wattam-Bell, "Normal and anomalous development of visual motion processing: motion coherence and dorsal-stream vulnerability'," Neuropsychologia **41**, 1769–1784 (2003).
19. M. Levi and R. S. Harwerth, "Spatio-temporal interactions in anisometropic and strabismic amblyopia," Invest. Ophthalmol. Visual Sci. **16**, 90–95 (1977).
20. R. F. Hess and E. R. Howell, "The threshold contrast sensitivity function in strabismic amblyopia: evidence for a two type classification," Vision Res. **17**, 1049–1055 (1977).
21. R. F. Hess, R. Demanins, and P. J. Bex, "A reduced motion aftereffect in strabismic amblyopia," Vision Res. **37**, 1303–1311 (1997).
22. R. F. Hess, T. D. France, and U. Tulunay-Keesey, "Residual vision in humans who have been monocularly deprived of pattern stimulation in early life," Exp. Brain Res. **44**, 295–311 (1981).
23. D. H. Brainard, "The Psychophysics Toolbox," Spatial Vis. **10**, 433–436 (1997).
24. D. G. Pelli, "The VideoToolbox software for visual psychophysics: transforming numbers into movies," Spatial Vis. **10**, 437–442 (1997).
25. D. G. Pelli and L. Zhang, "Accurate control of contrast on microcomputer displays," Vision Res. **31**, 1337–1350 (1991).
26. R. J. Watt and D. Andrews, "APE: adaptive estimates of psychometric functions," Curr. Psychol. Rev. **1**, 205–214 (1981).
27. F. A. Wichmann and N. J. Hill, "The psychometric function: I. Fitting, sampling, and goodness of fit," Percept. Psychophys. **63**, 1293–1313 (2001).
28. F. A. Wichmann and N. J. Hill, "The psychometric function: II. Bootstrap-based confidence intervals and sampling," Percept. Psychophys. **63**, 1314–1329 (2001).
29. S. C. Dakin, "Information limit on the spatial integration of local orientation signals," J. Opt. Soc. Am. A **18**, 1016–1026 (2001).
30. B. Mansouri, H. A. Allen, R. F. Hess, S. C. Dakin, and O. Ehrt, "Integration of orientation information in amblyopia," Vision Res. **44**, 2955–2969 (2004).
31. B. Mansouri, H. A. Allen, R. F. Hess, and S. C. Dakin, "Integration of global information in amblyopia and the effect of noise," presented at the Society for Neuroscience Annual Meeting, San Diego, Calif., October 23–27, 2004.
32. A. J. Simmers, T. Ledgeway, and R. F. Hess, "The influences of visibility and anomalous integration processes on the perception of global spatial form versus motion in human amblyopia," Vision Res. **45**, 449–460 (2005).
33. B. Mansouri, H. A. Allen, and R. F. Hess, "Detection, discrimination and integration of second-order orientation information in strabismic and anisometropic amblyopia," Vision Res. **45**, 2449–2460 (2005).
34. O. J. Braddick, J. M. O'Brien, J. Wattam-Bell, J. Atkinson, and R. Turner, "Form and motion coherence activate independent, but not dorsal/ventral segregated, networks in the human brain," Curr. Biol. **10**, 731–734 (2000).
35. B. Mansouri, R. F. Hess, H. A. Allen, and S. C. Dakin, "Integration, segregation, and binocular combination," J. Opt. Soc. Am. A **22**, 38–48 (2005).